ACS Photonics

Article

pubs.acs.org/journal/apchd5

Touching Gold Nanoparticle Chain Based Plasmonic Antenna Arrays and Optical Metamaterials

Zhongyang Li, Serkan Butun, and Koray Aydin*

Department of Electrical Engineering and Computer Science, Northwestern University, Evanston, Illinois 60208, United States

Supporting Information

ABSTRACT: The control of light−material interactions at the nanoscale requires optical elements with sizes much smaller than the wavelength of light. Plasmonic nanostructures and optical metamaterials enable drastic control and manipulation of light at such small scales. However it is quite challenging to further reduce the size of resonant elements using conventional plasmonic nanostructures. In this paper, we propose novel optical resonators that rely on the conducting plasmon mode of touching nanoparticle chains that enable significant size reduction when compared with widely used nanostripe antennas and U-shaped split-ring resonators. We employ full-field electromagnetic simulations to study the resonance mechanisms of nanoparticle chain arrays. In comparison with the nanobar plasmonic antennas, a nanoparticle chain based antenna with similar physical sizes operates at larger wavelengths, opening routes for deep subwavelength plasmonic resonators. Moreover, using nanoshell chain arrays, we demonstrate an optical resonator that is 10 times smaller than the resonance wavelength ($\lambda/10$). Similarly, nanoparticle-based split-ring resonators provide significant size reduction that could be used for smaller metamaterial and metasurface building blocks. Designing nanoparticle-based resonant elements is a promising route for achieving optical metamaterials with smoother resonance dispersion and lower optical losses.

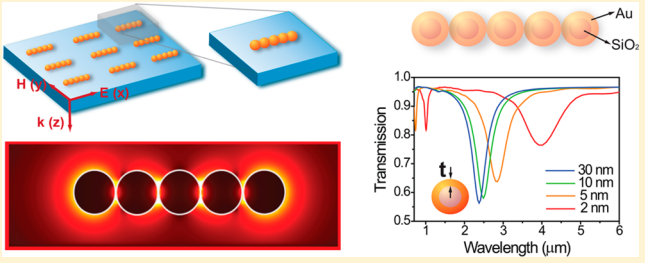

KEYWORDS: *localized surface plasmons, metamaterials, plasmonics, gold nanoparticle, nanoparticle chains*

Metal nanostructures support localized surface plasmon resonances at optical frequencies that can be controlled by the size, shape, and dielectric permittivity of the environment.[1−6] The field of plasmonics is dedicated to the study of optical properties of various metal nanostructures including chemically synthesized metal nanoparticles (bottom-up),[7] as well as top-down fabricated[8] metallic gratings, antennas, and nanostructure arrays, enabling strong light−material interactions such as enhanced scattering and absorption and highly localized electric fields. Similarly, optical metamaterials are composed of metal nanostructures with unique geometries, facilitating localized electric and/or magnetic resonances.[9−15] Initially, the fields of plasmonics and metamaterials progressed as two separate disciplines with very minimal overlap. However, after realization of optical metamaterials using plasmonic nanostructures, the interactions and exchange between the fields of plasmonics and metamaterials are increased drastically. Here, we propose novel metamaterial building blocks composed of metal nanoparticle chains that strongly benefit between the synergy of plasmonics and metamaterials.

Although localized surface plasmon resonances (LSPRs) of metallic nanoparticles are very effective in increasing the interactions between photons and materials, one can further enhance these interactions using coupled plasmonic nanoparticles,[5] such as dimers,[16−18] trimers,[19] and an even larger number of nanoparticles resulting in nanoclusters.[20−24] The distance between plasmonic nanoparticles turns out to be an extremely important parameter governing the coupling between the nanoparticles. Recently, numerous studies have revealed exciting quantum plasmonic effects for metal nanoparticles that are separated by a distance of 0.5 nm or below.[25−28] Although much attention has been devoted to dimers with ultrasmall gap distances, it is worth investigating what happens when particles are brought into contact. It has been shown that touching nanoparticles behave like a single nanoparticle that supports the conducting plasmon mode but not the hybridized resonance mode. Effectively, one can model the resulting nanostructure as a single nanoparticle rather than two individual nanoparticles. Touching nanoparticles and nanodisks have been also described in detail using coordinate transformation.[29,30]

In this article, we propose ultrasmall optically resonant elements based on touching nanoparticle chains with unique advantages over conventional top-down-fabricated plasmonic antennas and metamaterials. Electromagnetic wave simulations predict that the resonance wavelength of nanoparticle chain based metamaterial arrays are much larger than their counterparts that are formed from stripe and split-ring resonator arrays with the same physical size. Moreover, metal nanoparticle chain based metamaterials provide stronger field localization around the contact points, paving the way toward highly sensitive, ultracompact biosensors. We also extend our studies to

Received: October 21, 2013
Published: February 19, 2014

incorporate Au/SiO_2 nanoshells[31,32] into the metamaterial design, and we found that resonators designed with metallic nanoshells could further increase the resonance wavelength, therefore opening routes for deep subwavelength metamaterial building blocks at near- and mid-IR wavelengths.

RESULTS AND DISCUSSION

Using full-field electromagnetic simulations, we investigated several resonant antenna arrays that are composed of either metallic nanobar (Figure 1a) or touching nanoparticle chains

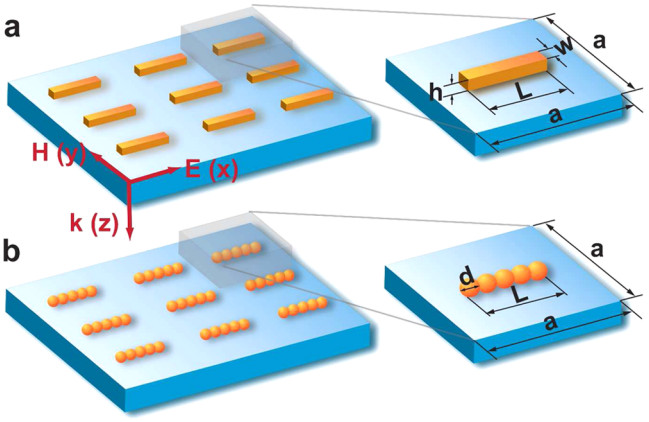

Figure 1. Three-dimensional configurations for nanobar (a) and NPC (b) arrays on a glass substrate. The lattice constant of arrays in both the *x*- and *y*-direction are a = 600 nm. The electromagnetic wave is normally incident to the metamaterial plane with the *E*-field polarized along the *x*-axis. (a) The width and height of the nanobar is $w = h$ = 60 nm, and the length is l = 180, 300, or 420 nm. (b) The diameter of each nanosphere is fixed at 60 nm. The number of nanoparticles in the chain is N = 3, 5, or 7, which corresponds to the same length as nanobars of $l_{N=3}$ =180 nm, $l_{N=5}$ = 300 nm, or $l_{N=7}$ = 420 nm, respectively.

(Figure 1b). In the simulations, we use periodic boundary conditions to study the resonance spectra. Nanobar antenna arrays[33] have been widely studied in the literature; here we report nanobar results for comparing the resonant behavior of touching nanoparticle chain arrays. In our design, the width and height of each nanobar is chosen to be $w = h$ = 60 nm, and arrays of nanobars with three different lengths are investigated: l = 180, 300, and 420 nm (Figure 1a). Nanobars are arranged periodically in the *xy*-plane with an in-plane periodicity of a = 600 nm in both directions. In all of the simulations, we assumed that the arrays are located on an optically thick glass substrate with a refractive index of n = 1.45. Figure 1b shows a three-dimensional configuration of nanoparticle chain (NPC) arrays in which gold nanoparticles are physically connected (touching) to neighboring nanoparticles. We have chosen the diameter of gold nanoparticles to be 60 nm, having the same width and height as those of the nanobar, therefore making the comparison easier. We have performed simulations for three different numbers of nanoparticle arrays, N = 3, 5, and 7. The number of nanoparticles is chosen such that the total lengths of NPCs and nanobars are the same. The lengths of individual NPCs along the polarization direction x are given as $l_{N=3}$ = 180 nm, $l_{N=5}$ = 300 nm, and $l_{N=7}$ = 420 nm.

We performed full-field electromagnetic simulations using a commercially available software package, Lumerical FDTD. For the complex refractive indices of Au, we used the Palik model,[34] whereas the refractive index of the substrate is assumed to be 1.45. The electromagnetic wave is propagating along the *z*-axis with the electric field polarized along the *x*-axis (Figure 1a). The transmission spectra for nanobar and NPC arrays are plotted in Figure 2a, b, and c, comparing the spectra for

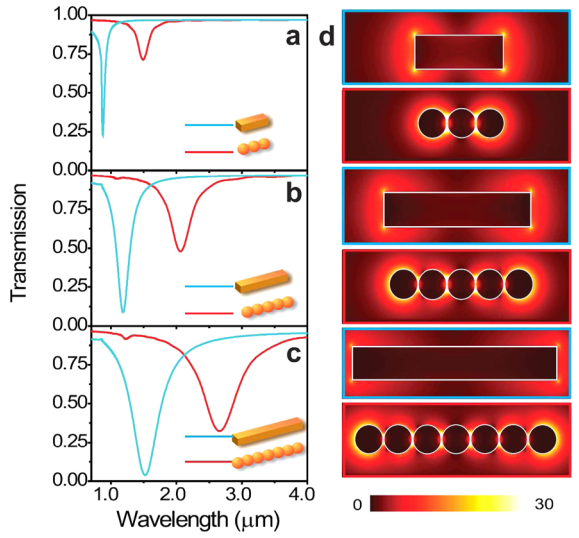

Figure 2. (a–c) Simulated transmission spectra of metallic nanobars (blue line) and NPC (red line) arrays with various length. Nanobars are chosen to have lengths of l = 180, 300, or 420 nm, whereas the number of nanoparticles in the chain is N = 3, 5, or 7, corresponding to the same length as that of nanobars of $l_{N=3}$ = 180 nm, $l_{N=5}$ = 300 nm, or $l_{N=7}$ = 420 nm, respectively (d) Map of *E*-field density distributions of nanobars and NPCs on the plane crossing the center of the nanostructures at respective resonances.

nanobars and NPCs of the same length l. When nanoparticles are touching each other, the contact between them serves as a "junction" for free electrons to flow from one nanoparticle to its neighbors.[35] Hence, rather than exhibiting hybridized plasmon modes for nontouching nanoparticles, the conductive plasmon modes of the nanoparticle chains are excited for this case.[36] To be specific, in the case of N = 3 where the total length is l = 180 nm, nanobar arrays display primarily a single well-pronounced resonance dip at 0.88 μm corresponding to the dipolar mode, whereas NPC arrays exhibit a resonant behavior at a higher wavelength, 1.49 μm (Figure 2a). Although the physical sizes of these two structures are comparable, there is a significant red-shift in the resonance wavelength. We observe a similar trend in Figure 2b and c, as the resonance wavelengths are shifting toward much higher wavelengths. Moreover, nanobar arrays with l = 300 nm give rise to a resonant dip at 1.18 μm, while NPC arrays of the same length are resonant at 2.06 μm (Figure 2b). With the higher number of nanoparticles, the difference between the resonant wavelengths of nanobars and NPCs is further increasing.

One can understand and interpret the resonance wavelength shift between nanobars and NPCs using a qualitative interpretation. The dipole resonance of optical antennas is well understood, as they scale up with the size of the antenna along the polarization direction due to the dipolar resonances. The external electric field causes charge oscillation along the optical antenna, and hence a metallic nanobar functions as a dipolar resonator. For nanoparticle chains, the charges are oscillating over a larger path, which is due to increased surface area in comparison with the rectangular nanobar shape, which

dx.doi.org/10.1021/ph4000828 | ACS Photonics 2014, 1, 228–234

in turns increases the resonance wavelength. Moreover, a much larger coupling capacitance is also provided by additional charge accumulation space in the junction between adjacent nanospheres. The drastic red-shift of the resonance between NPCs and nanobar arrays is therefore attributed to both increased surface area in the NPC arrays and also increased capacitance in the touching nanoparticle design. It is worth noting that the resonance wavelengths of three NPC (red line in Figure 2a) arrays with a physical length of 180 nm and nanobar arrays with l = 420 nm (blue line in Figure 2c) are comparable, enabling one to obtain similar resonance wavelengths by using a much smaller optical resonant element. Bringing nanoparticles together to form a conductive nanoparticle chain could enable smaller and more compact optical antennas and optical metasurface building blocks. In our simulations, we assumed that the nanoparticles touch each other at a single point contact; however in practical cases, the contact area would be larger due to faceted nanoparticle surfaces. We have performed additional simulations, shown in Figure S1 of the Supporting Information, indicating that the largest red-shift will be obtained when particles touch each other at a single point, and the amount of red-shift will decrease with increased contact area.

To more clearly illustrate the underling physics behind the spectra, the near E-field distributions for three different geometric dimensions are calculated. Figure 2d shows the total E-field intensity for both nanobars and NPCs at their corresponding resonance wavelengths. Electric field intensities are calculated at the center (30 nm above the glass surface) of nanobars and nanoparticle chains. In particular, NPCs are exhibiting much stronger field localization around the contact points, resulting in larger area hot spots when compared with that of the nanobars. Electromagnetic energy could be confined to the junctions between nanoparticles, giving rise to intense localized E-field "hot spots".[37,38] Enhanced local fields in nanoparticle-based resonators offer higher sensitivity dependence on structure geometry and the surrounding dielectric environment,[39] serving as possible ultrasmall building blocks for nanophotonic devices functioning as antennas, filters, or biosensors. In particular, strong resonances could be useful for surface-enhanced Raman spectroscopy (SERS) applications, which require high-field localization at both the excitation laser wavelengths and corresponding Raman-shift wavelengths.

In addition to gold nanoparticles, one can also envision using gold nanoshells for construction of nanoparticle chain based optical components. Touching nanoshell chains (NSCs) are also investigated as building blocks for plasmonic metamaterials.[31] An NSC molecule is made up of five gold nanoshells encapsulating silica cores, as schematically depicted in Figure 3a. Nanoshells with varying core and shell sizes offer dramatic control over the plasmonic response, in particular enabling to shift localized plasmon resonances to near-infrared wavelengths.[40,41] In our simulations, the diameter of nanoshells is fixed at 60 nm and the thickness of the gold shell region, t, is varied from 2 to 30 nm, where t = 30 nm is a gold nanoparticle, since there is no oxide core inside. Transmission spectra of NSCs with different shell thicknesses are plotted in Figure 3b. Similar to an observed red-shift from a transition of a nanoparticle to a nanoshell, touching nanoshell chain arrays demonstrate significant red-shift toward mid-infrared wavelengths. Even with a shell thickness of t = 2 nm, one can obtain a relatively strong resonant transmission dip with a resonance wavelength around 4 μm. Plasmonic nanoparticles and

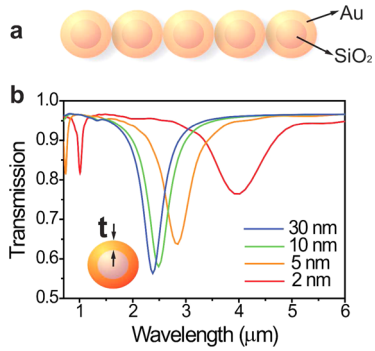

Figure 3. (a) Schematic representation of a single touching Au-shell/SiO_2-core nanoparticle chain (NSC). Five touching nanoshells with a diameter of 60 nm are brought into contact. (b) Transmission spectra of NSC arrays as a function of outer metallic layer thickness t.

nanoshells are mainly used for optical and plasmonic applications at the visible and near-IR wavelengths; however using our proposed nanoshell and nanoparticle chains, one can push the plasmon resonance wavelengths to mid-IR wavelengths. As the thickness of the metallic layer t is reduced, the interaction of the E-field and free electrons is restricted to the outer layer of the spheres. In this limit, the collective oscillation path of charges is taking place close to the sphere surface, resulting in a longer wavelength operation. Hence, nanoshell chain arrays offer significant size reduction in the size of optical antenna arrays from a conventional nanobar antenna of size/3 to an NSC-based antenna of size λ/10. In particular, nanoshell arrays could be designed for highly sensitive surface-enhanced infrared resonance absorption (SEIRA) sensors.[42−45]

In addition to the nanoparticle chain that serves as an optical antenna, one can utilize nanoparticle chains for more complex resonator designs. Here, we demonstrate a well-known resonator type, which is a U-shaped split-ring resonator[14,15] (USRR) and touching nanoparticle chain arranged to have a U-shape (UNPC). Split-ring resonators are widely studied for realizing metamaterials with electric and magnetic resonances. Figure 4a shows a single unit cell of a USRR with the following geometric parameters: the width and height of each branch of the USRR is w = h = 60 nm, its base length is l_x, and its arm length is l_y (both l_x and l_y can be tuned to $l_{N=3}$ =180 nm, $l_{N=5}$ = 300 nm, or $l_{N=7}$ = 420 nm). Similarly, UNPCs with the same size of l_x and l_y consist of touching nanoparticles whose diameter is 60 nm (Figure 4b). The period of each unit cell in the x- and y-direction is a = 600 nm. The plane wave source is normally incident onto the structure (k_z) with the E-field perpendicular to the arms (E_x) of both U-shaped resonators.

Figure 4c−e plot and compare the transmission spectra of USRR and UNPC arrays with varying base length (L_x): 180, 300, and 420 nm, respectively. In this case, the arm lengths (L_y) are kept the same. Two pronounced dips in the transmission spectra are observed in the simulations. The resonance dips at larger wavelengths correspond to the LC resonances of U-shaped resonators, in which the effective inductance, L_{eff}, depends on the total electrical length (L_x + 2L_y) of the resonators. In a USRR with its base and arm length of 300 nm (Figure 4d), the resonance at 2.43 μm corresponds to the LC resonance, characterized by a charge oscillation along the entire wire that forms the USRR; the other resonance at 1.00 μm is due to a dipolar resonance depending on the base of the USRR. Increasing the base length or the arm length in USRR and UNPC resonators increases the effective inductance of the

dx.doi.org/10.1021/ph4000828 | ACS Photonics 2014, 1, 228−234

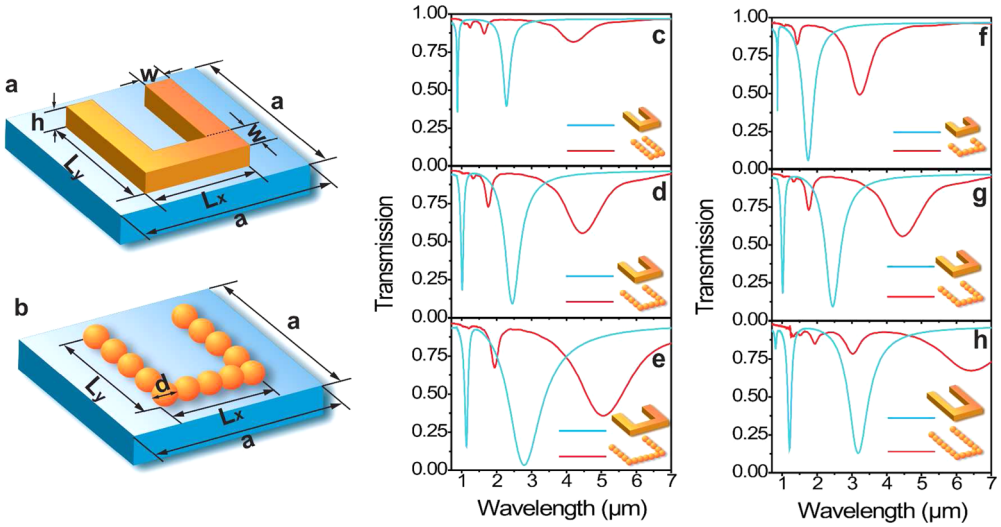

Figure 4. (a, b) Schematic configurations of USRR and UNPC building blocks. The period of the metamaterial in both the *x*- and *y*-direction is a = 600 nm. The source wave is normally incident to the structure plane with the *E*-field parallel to the gap of both U-shape resonators. (a) The width and height of each wire in the USRR are $w = h$ = 60 nm, with its base length l_x and arm length l_y. (b) The diameter of the spheres is d = 60 nm, and the number of nanoparticles in the base (N_x) or arm (N_y) is varied to be the same geometric length as the USRR. (c–f) Transmission spectra for USRRs (blue line) and UNPCs (red line) as a function of the base and arm length.

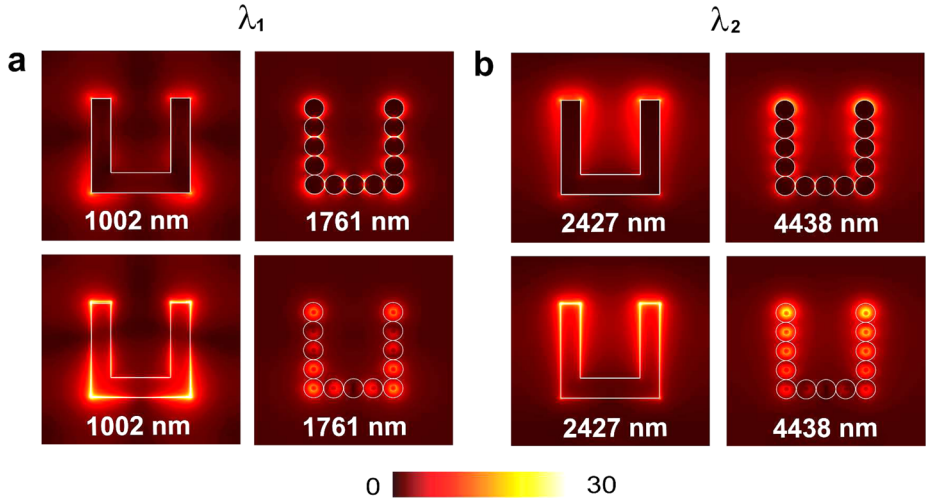

Figure 5. Localized *E*-field density distributions of USRRs and UNPCs at the plane crossing the center of the nanostructures (upper figures) and at the bottom plane (bottom figures) at respective resonances.

resonators, hence causing the LC resonance to red-shift. When the number of nanoparticles in a UNPC's base is increased from 3 to 7, the resonance wavelength is shifted by ∼1 μm to longer wavelengths. However, for USRR counterparts the resonance shift was only ∼0.5 μm. Although we observe a red-shift in both cases, nanoparticle chain based SRR resonators provide a larger amount of shift. Figure 4f − h plot the transmission spectra for varying USRR and UNPC arm lengths. We observe similar resonance behavior in the transmission spectra. In this case, the red-shift is even larger due to a larger increase in the effective inductance. We note that the resonance dips in the transmission spectra for UNPC arrays are at longer wavelengths when compared with the same USRR geometry. This is similar to the red-shift effect between nanobars and NPCs discussed previously. The largest spectral change between a USRR and UNPC with similar sizes is calculated to be as high as 3.25 μm in the case of Figure 4h. Such drastic size reduction is opening routes for designing ultrasmall building blocks for optical metamaterials and metasurfaces based on nanoparticle chains.

We plot the *E*-field distribution for USRRs and UNPCs at the resonance wavelengths λ_1 (dipolar mode) and λ_2 (LC resonance) in Figure 5a and b, respectively. The top section shows the field intensity at the center of the UNPCs and USRRs, i.e., z = 30 nm above the substrate, while the bottom section plots the field intensity at the metal–insulator interface (z = 0 nm) between the resonators and the substrate. The field intensity is highly localized around the base of the USRR for the dipole mode (λ_1) due to dipolar excitation of the electric field, whereas for the LC resonance, the field intensities are highly concentrated between the arms of the U-shape resonators. The confined *E*-field "hot spots" are localized near the touching points of nanoparticles, and this quite high field intensity has great potential for ultrasensitive biosensing.

Although the resonance wavelength is an important parameter in describing the optical resonances of optical

dx.doi.org/10.1021/ph4000828 | ACS Photonics 2014, 1, 228–234

antennas and metamaterials, it is worth exploring the effect of nanoparticle chains on the effective medium parameters. We calculated the real and imaginary parts of effective permittivity for nanobar and nanoparticle chains using the retrieval procedure.[46] Figure 6a plots and compares the effective

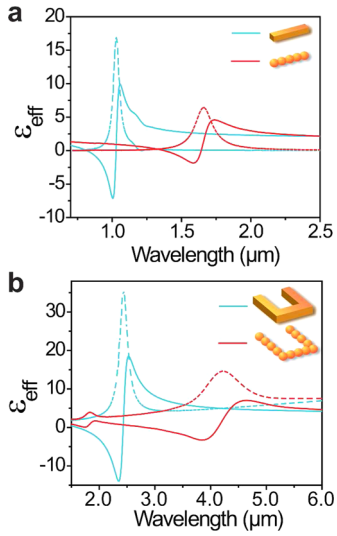

Figure 6. Retrieved effective permittivity for (a) nanobars and NPCs and (b) USRRs and UNPCs, respectively. Solid (dashed) curve represents the real (imaginary) part of the permittivity.

permittivity for nanobars and NPC resonator arrays. We observe a resonant behavior in the effective permittivity near the resonance wavelength, where the effective permittivity takes negative values. While metamaterials with nanobars have a sharp transition, we note that the nanoparticle-based metamaterials possess a smoother transition. In particular, it is worth mentioning that the epsilon-near-zero region is broader in wavelength scale for nanoparticle-based metamaterials (Figure 6b). Moreover, nanoparticle-based metamaterials reveal a smaller imaginary part of permittivity, therefore exhibiting lower losses around the resonance frequency. In addition to the significant size reduction, nanoparticle-based optical resonators and metamaterials could exhibit smoother resonance dispersion and lower optical losses. That is because the external electric field could drive and excite the charge oscillation along the nanobar antenna far more strongly since the bulk resonator provides a larger cross-section area for the electron flow, which leads to stronger excitation of the dipolar resonance. However, in the case of an NPC, the small contact region between nanoparticles critically restricts the intensity of charge oscillation through the chain due to the very limited cross-section area of the junction.

Such nanoparticle chain based optical components can be fabricated by combining the top-down fabrication of substrates with the bottom-up assembly of nanoparticle chains.[19,23] There is a growing interest in fabricating coupled nanoparticles with smaller gap sizes and even touching in the literature. Recently, SERS enhancement from two touching nanoparticles has been experimentally reported, where the authors functionalize nanoparticles with reported molecules and then they are slightly aggregated.[47] As an alternative method, one could align nanoparticles on a substrate using a top-down fabrication approach such as electron-beam lithography, and gold nanoparticles might be overgrown to ensure that the particles are touching. Another possible method would be to arrange nanoparticles on a strained flexible substrate and relax the substrate to bring the nanoparticles into physical contact.[48] It is also worth noting that designing optical elements based on nanoparticles will also help reduce the losses due to surface roughnesses of deposited metal nanostructures, which is a significant drawback for top-down fabrication processes. Since nanoparticles can be synthesized to have single-crystalline form, nanoparticle chain arrays are expected to have much fewer optical losses due to smoother surfaces.

CONCLUSIONS

In conclusion, we have proposed ultrasmall building blocks of plasmonic antennas and optical metamaterials based on touching nanoparticle chains with deep subwavelength size on the order of $\lambda/10$. Such linear nanoparticle chains can be fabricated using templated assembly onto a lithographically defined substrate with high yields.[19−21,49] It is also possible to control the structural geometry and engineer specific plasmon modes using a different lithographic template. We have demonstrated that touching nanoparticle chain arrays could drastically reduce the dimensions of conventional antennas from $\lambda/3$ to $\lambda/10$, enabling ultrasmall optical resonant elements for antennas, filters, and biosensors. High localized field concentration near the contact points of nanoparticles can be used as very sensitive biological sensors. Moreover, one can design more complex resonant elements such as U-shaped resonators using nanoparticle chain arrays. The effective permittivity of optical metamaterials reveals smoother dispersion in the epsilon-near-zero region with smaller optical losses.

ASSOCIATED CONTENT

Supporting Information

Spectral evolution of nonideal nanoparticle chains with faceted contact due to synthesis and fabrication challenges; spectral comparison in energy scale; angle-dependence of NPC arrays. This information is available free of charge via the Internet at http://pubs.acs.org.

AUTHOR INFORMATION

Corresponding Author

*E-mail: aydin@northwestern.edu.

Notes

The authors declare no competing financial interest.

ACKNOWLEDGMENTS

This material is based upon work supported by the AFOSR under Award No. FA9550-12-1-0280. K.A. acknowledges financial support from the McCormick School of Engineering and Applied Sciences at Northwestern University and partial support from the Institute for Sustainability and Energy at Northwestern (ISEN) through an ISEN Booster Award.

REFERENCES

(1) Maier, S. A.; Brongersma, M. L.; Kik, P. G.; Meltzer, S.; Requicha, A. A. G.; Atwater, H. A. Plasmonics—a route to nanoscale optical devices. *Adv. Mater.* **2001**, *13*, 1501−1505.

(2) Barnes, W. L.; Dereux, A.; Ebbesen, T. W. Surface plasmon subwavelength optics. *Nature* **2003**, *424*, 824−830.

(3) Ozbay, E. Plasmonics: merging photonics and electronics at nanoscale dimensions. *Science* **2006**, *311*, 189−193.

(4) Lal, S.; Link, S.; Halas, N. J. Nano-optics from sensing to waveguiding. *Nat. Photonics* **2007**, *1*, 641−648.
(5) Halas, N. J.; Lal, S.; Chang, W. S.; Link, S.; Nordlander, P. Plasmons in strongly coupled metallic nanostructures. *Chem. Rev.* **2011**, *111*, 3913−3961.
(6) Luk'yanchuk, B.; Zheludev, N. I.; Maier, S. A.; Halas, N. J.; Nordlander, P.; Giessen, H.; Chong, C. T. The Fano resonance in plasmonic nanostructures and metamaterials. *Nat. Mater.* **2010**, *9*, 707−715.
(7) Hoeppener, S.; Maoz, R.; Cohen, S. R.; Chi, L.; Fuchs, H.; Sagiv, J. Metal nanoparticles, nanowires, and contact electrodes self-assembled on patterned monolayer templates−a bottom-up chemical approach. *Adv. Mater.* **2002**, *14*, 5.
(8) Tong, H. D.; Chen, S.; van der Wiel, W. G.; Carlen, E. T.; van den Berg, A. Novel top-down wafer-scale fabrication of single crystal silicon nanowires. *Nano Lett.* **2009**, *9*, 1015−1022.
(9) Smith, D.; Pendry, J.; Wiltshire, M. Metamaterials and negative refractive index. *Science* **2004**, *305*, 788−792.
(10) Liu, N.; Guo, H.; Fu, L.; Kaiser, S.; Schweizer, H.; Giessen, H. Three-dimensional photonic metamaterials at optical frequencies. *Nat. Mater.* **2007**, *7*, 31−37.
(11) Schurig, D.; Mock, J.; Justice, B.; Cummer, S.; Pendry, J.; Starr, A.; Smith, D. Metamaterial electromagnetic cloak at microwave frequencies. *Science* **2006**, *314*, 977−980.
(12) Linden, S.; Enkrich, C.; Wegener, M.; Zhou, J.; Koschny, T.; Soukoulis, C. M. Magnetic response of metamaterials at 100 terahertz. *Science* **2004**, *306*, 1351−1353.
(13) Rockstuhl, C.; Zentgraf, T.; Guo, H.; Liu, N.; Etrich, C.; Loa, I.; Syassen, K.; Kuhl, J.; Lederer, F.; Giessen, H. Resonances of split-ring resonator metamaterials in the near infrared. *Appl. Phys. B: Laser Opt.* **2006**, *84*, 219−227.
(14) Pryce, I. M.; Aydin, K.; Kelaita, Y. A.; Briggs, R. M.; Atwater, H. A. Highly strained compliant optical metamaterials with large frequency tunability. *Nano Lett.* **2010**, *10*, 4222−4227.
(15) Dicken, M. J.; Aydin, K.; Pryce, I. M.; Sweatlock, L. A.; Boyd, E. M.; Walavalkar, S.; Ma, J.; Atwater, H. A. Frequency tunable near-infrared metamaterials based on VO2 phase transition. *Opt. Express* **2009**, *17*, 18330−18339.
(16) Tabor, C.; Van Haute, D.; El-Sayed, M. A. Effect of orientation on plasmonic coupling between gold nanorods. *ACS Nano* **2009**, *3*, 3670−3678.
(17) Brown, L. V.; Sobhani, H.; Lassiter, J. B.; Nordlander, P.; Halas, N. J. Heterodimers: plasmonic properties of mismatched nanoparticle pairs. *ACS Nano* **2010**, *4*, 819−832.
(18) Prodan, E.; Radloff, C.; Halas, N.; Nordlander, P. A hybridization model for the plasmon response of complex nanostructures. *Science* **2003**, *302*, 419−422.
(19) Fan, J. A.; Wu, C.; Bao, K.; Bao, J.; Bardhan, R.; Halas, N. J.; Manoharan, V. N.; Nordlander, P.; Shvets, G.; Capasso, F. Self-assembled plasmonic nanoparticle clusters. *Science* **2010**, *328*, 1135−1138.
(20) Slaughter, L. S.; Willingham, B. A.; Chang, W.-S.; Chester, M. H.; Ogden, N.; Link, S. Toward plasmonic polymers. *Nano Lett.* **2012**, *12*, 3967−3972.
(21) Barrow, S. J.; Wei, X.; Baldauf, J. S.; Funston, A. M.; Mulvaney, P. The surface plasmon modes of self-assembled gold nanocrystals. *Nat. Commun.* **2012**, *3*, 1275.
(22) Urban, A. S.; Shen, X.; Wang, Y.; Large, N.; Wang, H.; Knight, M. W.; Nordlander, P.; Chen, H.; Halas, N. J. Three-dimensional plasmonic nanoclusters. *Nano Lett.* **2013**, *13*, 4399−4403.
(23) Fafarman, A. T.; Hong, S. H.; Caglayan, H.; Ye, X. C.; Diroll, B. T.; Paik, T.; Engheta, N.; Murray, C. B.; Kagan, C. R. Chemically tailored dielectric-to-metal transition for the design of metamaterials from nanoimprinted colloidal nanocrystals. *Nano Lett.* **2013**, *13*, 350−357.
(24) Rahmani, M.; Lei, D. Y.; Giannini, V.; Lukiyanchuk, B.; Ranjbar, M.; Liew, T. Y. F.; Hong, M. H.; Maier, S. A. Subgroup decomposition of plasmonic resonances in hybrid oligomers: modeling the resonance lineshape. *Nano Lett.* **2012**, *12*, 2101−2106.
(25) Ciracì, C.; Hill, R.; Mock, J.; Urzhumov, Y.; Fernández-Domínguez, A.; Maier, S.; Pendry, J.; Chilkoti, A.; Smith, D. Probing the ultimate limits of plasmonic enhancement. *Science* **2012**, *337*, 1072−1074.
(26) Scholl, J. A.; Koh, A. L.; Dionne, J. A. Quantum plasmon resonances of individual metallic nanoparticles. *Nature* **2012**, *483*, 421−427.
(27) Lassiter, J. B.; Aizpurua, J.; Hernandez, L. I.; Brandl, D. W.; Romero, I.; Lal, S.; Hafner, J. H.; Nordlander, P.; Halas, N. J. Close encounters between two nanoshells. *Nano Lett.* **2008**, *8*, 1212−1218.
(28) Tosi, G.; Christmann, G.; Berloff, N.; Tsotsis, P.; Gao, T.; Hatzopoulos, Z.; Savvidis, P.; Baumberg, J. Geometrically locked vortex lattices in semiconductor quantum fluids. *Nat. Commun.* **2012**, *3*, 1243.
(29) Pendry, J.; Aubry, A.; Smith, D.; Maier, S. Transformation optics and subwavelength control of light. *Science* **2012**, *337*, 549−552.
(30) Aubry, A.; Lei, D. Y.; Maier, S. A.; Pendry, J. Interaction between plasmonic nanoparticles revisited with transformation optics. *Phys. Rev. Lett.* **2010**, *105*, 233901.
(31) Perez-Gonzalez, O.; Zabala, N.; Borisov, A.; Halas, N.; Nordlander, P.; Aizpurua, J. Optical spectroscopy of conductive junctions in plasmonic cavities. *Nano Lett.* **2010**, *10*, 3090−3095.
(32) Wang, H.; Brandl, D. W.; Le, F.; Nordlander, P.; Halas, N. J. Nanorice: a hybrid plasmonic nanostructure. *Nano Lett.* **2006**, *6*, 827−832.
(33) Cubukcu, E.; Kort, E. A.; Crozier, K. B.; Capasso, F. Plasmonic laser antenna. *Appl. Phys. Lett.* **2006**, *89*, 093120.
(34) Palik, E. D. *Handbook of Optical Constants of Solids: Index*; accessed online via Elsevier, 1998; Vol. 3.
(35) Liu, H.; Genov, D.; Wu, D.; Liu, Y.; Steele, J.; Sun, C.; Zhu, S.; Zhang, X. Magnetic plasmon propagation along a chain of connected subwavelength resonators at infrared frequencies. *Phys. Rev. Lett.* **2006**, *97*, 243902.
(36) Atay, T.; Song, J.-H.; Nurmikko, A. V. Strongly interacting plasmon nanoparticle pairs: from dipole-dipole interaction to conductively coupled regime. *Nano Lett.* **2004**, *4*, 1627−1631.
(37) Nordlander, P.; Oubre, C.; Prodan, E.; Li, K.; Stockman, M. Plasmon hybridization in nanoparticle dimers. *Nano Lett.* **2004**, *4*, 899−903.
(38) Sainidou, R.; García de Abajo, F. J. Plasmon guided modes in nanoparticle metamaterials. *Opt. Express* **2008**, *16*.
(39) Eustis, S.; El-Sayed, M. A. Why gold nanoparticles are more precious than pretty gold: noble metal surface plasmon resonance and its enhancement of the radiative and nonradiative properties of nanocrystals of different shapes. *Chem. Soc. Rev.* **2006**, *35*, 209−217.
(40) Oldenburg, S.; Averitt, R.; Westcott, S.; Halas, N. Nano-engineering of optical resonances. *Chem. Phys. Lett.* **1998**, *288*, 243−247.
(41) Averitt, R. D.; Sarkar, D.; Halas, N. J. Plasmon resonance shifts of Au-coated Au_{2}S nanoshells: insight into multicomponent nanoparticle growth. *Phys. Rev. Lett.* **1997**, *78*, 4217−4220.
(42) Le, F.; Brandl, D. W.; Urzhumov, Y. A.; Wang, H.; Kundu, J.; Halas, N. J.; Aizpurua, J.; Nordlander, P. Metallic nanoparticle arrays: a common substrate for both surface-enhanced Raman scattering and surface-enhanced infrared absorption. *ACS Nano* **2008**, *2*, 707−718.
(43) Cubukcu, E.; Zhang, S.; Park, Y.-S.; Bartal, G.; Zhang, X. Split ring resonator sensors for infrared detection of single molecular monolayers. *Appl. Phys. Lett.* **2009**, *95*, 043113.
(44) Neubrech, F.; Pucci, A.; Cornelius, T. W.; Karim, S.; García-Etxarri, A.; Aizpurua, J. Resonant plasmonic and vibrational coupling in a tailored nanoantenna for infrared detection. *Phys. Rev. Lett.* **2008**, *101*, 157403.
(45) Aksu, S.; Yanik, A. A.; Adato, R.; Artar, A.; Huang, M.; Altug, H. High-throughput nanofabrication of infrared plasmonic nanoantenna arrays for vibrational nanospectroscopy. *Nano Lett.* **2010**, *10*, 2511−2518.
(46) Smith, D.; Schultz, S.; Markoš, P.; Soukoulis, C. Determination of effective permittivity and permeability of metamaterials from reflection and transmission coefficients. *Phys. Rev. B* **2002**, *65*, 195104.

(47) Kleinman, S. L.; Sharma, B.; Blaber, M. G.; Henry, A. I.; Valley, N.; Freeman, R. G.; Natan, M. J.; Schatz, G. C.; Van Duyne, R. P. Structure enhancement factor relationships in single gold nanoantennas by surface-enhanced raman excitation spectroscopy. *J. Am. Chem. Soc.* **2013**, *135*, 301−308.
(48) Ross, B. M.; Wu, L. Y.; Lee, L. P. Omnidirectional 3D nanoplasmonic optical antenna array via soft-matter transformation. *Nano Lett.* **2011**, *11*, 2590−2595.
(49) Chang, W.-S.; Slaughter, L. S.; Khanal, B. P.; Manna, P.; Zubarev, E. R.; Link, S. One-dimensional coupling of gold nanoparticle plasmons in self-assembled ring superstructures. *Nano Lett.* **2009**, *9*, 1152−1157.